Heliyon 10 (2024) e23168

Contents lists available at ScienceDirect

Heliyon

journal homepage: www.cell.com/heliyon

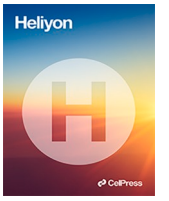

Exosome-derived miR-23a-5p inhibits HCC proliferation and angiogenesis by regulating PRDX2 expression MiR-23a-5p/PRDX2 axis in HCC progression

Yang Zhao [a,1], Jun Liu [b,1], Zhengping Xiong [a], Shanzhi Gu [a,*], Xibin Xia [b,**]

[a] *Department of Interventional Therapy, Hunan Cancer Hospital, The Affiliated Cancer Hospital of Xiangya School of Medicine, Central South University, 283 Tongzipo Road, Yuelu District, Changsha, 410006, Hunan, China*

[b] *Department of Radiology, Hunan Cancer Hospital, The Affiliated Cancer Hospital of Xiangya School of Medicine, Central South University, Changsha, 410006, Hunan, China*

ARTICLE INFO

Keywords:
miR-23a-5p
PRDX2
Exosomes
Angiogenesis
Hepatocellular carcinoma

ABSTRACT

microRNAs (miRNAs) are closely related to the progression of hepatocellular carcinoma (HCC). Cancer-derived exosomes play an essential role in the establishment of the HCC microenvironment. However, the possible effects and underlying mechanisms of exosome (exo) microRNA-23a-5p (miR-23a-5p) in the progression of HCC remain unknown. In this study, we aimed to determine the role and specific molecular mechanism of exo miR-23a-5p in regulating HCC progression and to investigate whether exo miR-23a-5p levels can serve as an indicator of the prognosis of transarterial chemoembolization in patients with HCC. Our findings illustrated that miR-23a-5p was downregulated in exosomes separated from the serum of HCC patients and that miR-23a-5p carried by exosomes inhibited HCC cell proliferation and angiogenesis. Mechanistically, miR-23a-5p negatively targeted peroxiredoxin-2 (PRDX2). Functionally, PRDX2 overexpression relieved exosome-induced inhibition of HCC cell proliferation and angiogenesis by promoting vascular endothelial growth factor (VEGF) expression. In conclusion, Exo miR-23a-5p inhibited HCC proliferation and angiogenesis by regulating PRDX2 expression. Our results revealed the role and specific molecular mechanism of exo miR-23a-5p in regulating HCC progression.

1. Introduction

HCC is a common malignant tumor that is the second most common cause of cancer-related death worldwide. HCC remains a global health challenge because of its high morbidity and mortality [1,2]. Because of the high clinical and biological heterogeneity of the tumor, HCC is often detected at an advanced stage, and patients miss the optimal treatment period [3]. Therefore, it is necessary to explore new detection biomarkers.

Exosomes are uniform vesicles secreted by cells with a diameter of 40–100 nm that were initially considered cell waste [4]. Exosomes were discovered in 1983 and gradually became a research hotspot until the beginning of the 21st century [5]. Exosomes are distributed in a variety of body fluids, such as blood, lymph, and urine. Exosomes can carry a variety of biological small molecules,

* Corresponding author.
** Corresponding author.
E-mail addresses: 171761993@qq.com (S. Gu), xiaxibin@hnca.org.cn (X. Xia).
[1] These authors contributed equally to this work and should be considered co-first authors

https://doi.org/10.1016/j.heliyon.2023.e23168
Received 18 May 2023; Received in revised form 22 November 2023; Accepted 28 November 2023
Available online 2 December 2023

such as proteins, lipids, mRNAs and miRNAs, and play a vital role in the information exchange between cells [6,7]. Currently, in many experiments, exosomes have become the best choice for high-quality carriers because of their relatively stable existence in the human body and the ability to escape human immune responses [8]. In fact, exosomes can participate in many physiological and pathological processes in the body, including antigen expression, cell migration, and tissue damage repair, and the specific functions of exosomes are determined by the type of cells they come from Refs. [9,10]. In addition, exosomes play a vital role in tumorigenesis, invasion and metastasis [11,12]. Therefore, in this study, we hypothesized that tumor-derived bioactive substances were transported into vascular endothelial cells via exosomes and then activated vascular endothelial cells to regulate angiogenesis and eventually regulate HCC progression.

miRNAs are noncoding RNA sequences that are approximately 18–22 base pairs in length [13]. Studies have shown that miRNAs play a vital role in gene expression by regulating posttranscriptional translation, which is somewhat linked to disease progression [14]. Increasing evidence indicates that tumor-derived exosomes often transfer miRNAs to recipient cells to induce the regulation of target genes. For example, tumor-derived exosomal miR-934 targets CXCL13 to promote the metastasis of colorectal cancer [15]. Moreover, it has been reported that miR-23a-5p was downregulated in HCC cell lines, and miR-23a-5p overexpression inhibited HCC cell metastasis [16], indicating that miR-23a-5p plays a negative role in HCC progression. Interestingly, our research preliminarily suggested that compared with that 1 day before transcatheter arterial chemoembolization (TACE), miR-23a-5p was upregulated in exosomes that were separated from the serum of HCC patients 3 days after TACE. Therefore, in this study, we hypothesized that tumor-derived miR-23a-5p may participate in the regulation of HCC progression. However, the specific mechanism remains unclear.

PRDX2 is a member of the PRDX family, which is highly expressed in many cancers, and compared with patients with low expression, patients with high expression of PRDX2 have a poor prognosis [17]. Under normal physiological conditions, the level of reactive oxygen species (ROS) is strictly controlled to maintain basic biological function and normal cell homeostasis [18]. The tumor-promoting effect of PRDX2 may be attributed to the protection of tumor cells from oxidative stress [19]. Therefore, we analyzed the association between ROS levels and HCC progression. In addition, studies have shown that PRDX2 promotes VEGF expression in cardiomyocytes under hypoxia, which in turn promotes angiogenesis and myocardial hypertrophy [20]. Moreover, at the beginning of the study, we found that there were binding sites between miR-23a-5p and PRDX2 by using TargetScan prediction. Therefore, we hypothesized that miR-23a-5p regulated VEGF expression by targeting PRDX2 in HCC. However, the specific molecular mechanism has yet to be elucidated.

In summary, exosomes adjust the tumor microenvironment by changing the physiological state of target cells. Therefore, exosomes are vital messengers in tumor progression. In this study, we first collected the serum of 12 patients with HCC before TACE and 3 days after TACE. It was found that the exo miR-23a-5p in serum 3 days after TACE was significantly higher than that before the operation. Subsequently, we collected and analyzed the serum of 110 HCC patients and found that miR-23a-5p was an independent predictor of overall survival (OS) and progression-free survival (PFS), and miR-23a-5p overexpression may inhibit the proliferation and angiogenesis of HCC cells. Therefore, we speculate that miR-23a-5p has a certain research value in the treatment of HCC. Our study demonstrated, the role and specific molecular mechanism of exo miR-23a-5p in regulating HCC progression. Exo miR-23a-5p may be a potential target for the treatment of HCC.

2. Materials and methods

2.1. Tissues and samples

According to the American Association for the Study of Liver Disease (AASLD) practice guidelines, first, the serum of 12 HCC patients before TACE and 3 days after TACE was collected, and exosomes were separated. Subsequently, the levels of miRNAs, including miR-23a-5p, miR-155-3p, miR-135b, miR-130b-3p and miR-210-3p, were measured by qRT−PCR. Furtherly, 110 patients with HCC were included in the study in our hospital between September 2020 and October 2021. Notably, the patients did not received

Table 1
The correlation between clinicopathological features and miR-23a-5p expression in 110 HCC patients.

Clinicopathologic features	miR-23a-5p expression		*P* value
	High (n = 58)	Low (n = 52)	
Gender (male, female)	36/22	33/19	0.863
Age (<60, ≥60)	22/36	26/26	0.435
Maximum tumor size (≤10 cm, >10 cm)	41/17	24/28	0.012*
BCLC stage (A, B, C)	2/31/25	18/21/13	0.008**
Tumor number (N)(1, >1)	24/34	25/27	0.565
ALT (U/L)(≤40, >40)	43/15	25/27	0.021*
AST (U/L)(≤40, >40)	39/19	24/28	0.034*
ALB (g/L)(≤35, >35)	35/23	39/13	0.109
PT (s) (≤13, >13)	33/25	18/34	0.023*
AFP (ng/ml) (≤20, 20–200, ≥200)	11/15/32	16/8/28	0.223

BCLC = Barcelona Clinic Liver Cancer; ALT = alanine aminotransferase; AST = aspartate aminotransferase; ALB = albumin; PT = prothrombin time; AFP = α-fetoprotein.
*$P < 0.05$ indicates a statistically significant difference.

anti-tumor treatment for HCC before TACE. All the protocols were approved by the Ethics Committee of Hunan Cancer Hospital, The Affiliated Cancer Hospital of Xiangya School of Medicine, Central South University. Each participant provided written informed consent to participate. The 110 patients' sex, age, maximum tumor size, Barcelona Clinic Liver Cancer (BCLC) stage, tumor number, ALT, AST, ALB, PT and AFP were recorded in detail (Table 1).

2.2. Exosome isolation and identification

The serum of patients with HCC days was collected and centrifuged at 300×*g* for 10 min, and the supernatant was assimilated. The supernatant was centrifuged at 2000×*g* (10 min) and 10,000×*g* (30 min) to remove the shedding vesicles. The supernatant was further removed by ultracentrifugation at 140,000×*g* for 90 min, and the resulting pellet was exosomes. The pellet was washed with PBS buffer, resuspended, centrifuged at 140,000×*g* for 90 min, resuspended in 100 μL of PBS buffer, and frozen at −80 °C for later use. Exosomes obtained by ultracentrifugation were added to PBS buffer (final concentration of 0.5 mg/mL) for identification. The exposure suspension was dropped on a copper plate, placed on filter paper, and then illuminated with an incandescent lamp for 10 min. The plate was incubated with 1% phosphotungstic acid for 5 min and light for 20 min and observed with a transmission electron microscope (FEI TECNAI G20, USA). According to the manufacturer's instructions, the size and distribution of the exosomes were analyzed using Tunable Resistive Pulse Sensing on qNano (Izon Science Ltd, Christchurch, New Zealand). Then, 100 μL of PBS buffer (final concentration of 0.5 mg/mL) containing exosomes was cocultured with HepG2 and SKHep-1 cells for 24 h. Treated HepG2 and SKHep-1 cells were used for subsequent experiments.

2.3. Cell lines and culture

Human umbilical vein endothelial cells (HUVECs), human hepatic stellate cell LX2 (CL-0560) and HCC cell Huh-7 (CL-0120) were provided by Pricella (Wuhan, China). ATCC (Manassas, VA, USA) provided HCC cell lines, including HepG2 (HB-8065), Hep3B (HB-8064) and SKHep-1 (HTB-52), and DMEM (Invitrogen, California, USA) containing 5% fetal bovine serum, 1% endothelial cell growth supplement and 1% penicillin/streptomycin solution (FBS, Gibco, NY, USA) was used to culture cells. All cells were cultured in a humid incubator at 37 °C and 5% CO_2. Cells were treated with *N*-Acetylcysteine (5 μM) for 30 min.

2.4. Cell treatment

The miR-23a-5p inhibitor and its negative control inhibitor NC, miR-32a-5p mimic and its negative control NC mimic were generated by Shanghai Jima Pharmaceutical Technology Co., Ltd. (Shanghai, China). The full-length sequences of PRDX2 were inserted into pcDNA3.1 (Invitrogen) for oe-PRDX2, and its negative control, oe-NC, was obtained in the same way. Corresponding plasmids were transfected into HUVECs, HepG2 and SKHep-1 cells by using Lipofectamine™ 3000 Transfection Reagent (Invitrogen).

2.5. qRT−PCR

Total RNA was extracted from HepG2 and SKHep-1 cells with TRIzol reagent (Invitrogen) as directed. Reverse transcribe 1 μg of total RNA into complementary DNA with the PrimeScrip RT kit. The mRNA levels of genes were measured with SYBR PreMix Ex Taq on the 7500 real-time fluorescence polymerase chain reaction system. GAPDH was used as an endogenous control for data analysis. MiRNAs were collected with the MirVana microRNA isolation kit (Invitrogen, AM1561). miRNA levels were measured with the TaqMan microRNA assay kit (Thermo Fisher, 4427975) with U6 RNA as an endogenous control. The data were calculated using the $2^{-\Delta\Delta CT}$ method. The primers used in this study are shown in Table 2.

Table 2
Primer sequences.

Primer name	Primer sequences
F-miR-23a-5p	5′-TTCCTGGGGATGGGATT -3′
R-miR-23a-5p	5′-GAACATGTCTGCGTATCTC -3′
F-miR-155-3p	5′-TGCTAATCGTGATAGGGG -3′
R-miR-155-3p	5′-GAACATGTCTGCGTATCTC -3′
F-miR-135b	5′-GGCTTTTCATTCCTATGTG -3′
R-miR-135b	5′-GAACATGTCTGCGTATCTC -3′
F-miR-130b-3p	5′-CTCTTTCCCTGTTGCAC -3′
R-miR-130b-3p	5′-GAACATGTCTGCGTATCTC -3′
F-miR-210-3p	5′-TGTGCGTGTGACAGCG -3′
R-miR-210-3p	5′-GAACATGTCTGCGTATCTC -3′
F-PRDX2	5′-CCTTCCAGTACACAGACGAGCA -3′
R-PRDX2	5′-CTCACTATCCGTTAGCCAGCCT -3′
F-U6	5′-CTCGCTTCGGCAGCACAT -3′
R-U6	5′-TTTGCGTGTCATCCTTGCG -3′
F-GAPDH	5′-GTCTCCTCTGACTTCAACAGCG -3′
R-GAPDH	5′-ACCACCCTGTTGCTGTAGCCAA -3′

2.6. MTT assay

Cells were suspended in DMEM culture medium containing 5 μg/mL MTT tetramethylazole salt (Sigma–Aldrich, USA) and incubated at 37 °C for 4 h. Dimethyl sulfoxide was added, and absorbance was determined by a microplate instrument at 490 nm (Beijing, China).

2.7. Colony formation assay

HepG2 and SKHep-1 cell single-cell suspensions were seeded in 15 mm dishes. After 14 days of culture, cells were fixed with 4% paraformaldehyde and stained with crystal violet. Subsequently, colonies consisting of more than 50 single cells were counted under a microscope for quantitative analysis.

2.8. Tube formation assay

First, the Transwell chamber (0.4-μm pore, Corning, New York, USA) was placed in a 6-well plate. HepG2 and SKHep-1 cells were placed in the upper compartment, and HUVECs were added to the compartment. After the cells were cocultured for 48 h, HepG2 and SKHep-1 cells were seeded in Matrigel-coated 96-well plates at a density of 1.5×10^4 cells per well. After 6 h, pictures were taken with a light microscope (Olympus, Tokyo, Japan), and the Angiogenesis Analyzer plugin of ImageJ was used to count the total length.

2.9. Enzyme-linked immunosorbent assay (ELISA)

Supernatants of HepG2 and SKHep-1 cells were collected after centrifugation for 10 min. Malondialdehyde (MDA, EU2577) and superoxide dismutase (SOD, EH4706-1) levels were measured using ELISA kits (FineTest, Wuhan, China) according to the manufacturers instructions. Absorbance at 450 nm was measured using a microplate reader (PerkinElmer, Waltham, MA, USA).

2.10. 2′,7′-dichlorodihydrofluorescein diacetate (DCFH-DA) staining

After 24 h of incubation of HepG2 and SKHep-1 cells with 0, 15, or 30 mM formate, the supernatant was removed, and the cells were washed three times with PBS. The cells were then harvested and suspended in PBS. Subsequently, DCFH-DA (10 μM) was added to the cells and incubated at 37 °C for 15 min. Finally, the fluorescence intensity (FL-1, 530 nm) of 10^4 cells was detected by using flow cytometry (FACSCalibur, BD Biosciences) to measure ROS generation.

2.11. Bioinformatics analysis and dual-luciferase reporter gene assay

Utilize the bioinformatics software TargetScan (www.Target-scan.org) predicted potential binding sites for miR-23a-5p and PRDX2. PGL3 vectors containing wild-type 3′-noncoding regions (PRDX2-WT) and mutant fragments (PRDX2-MUT) were cotransfected with pGL3 with HepG2 and SKHep-1 with Lipofectamine™ 3000 Transfection Reagent (Invitrogen). After 48 h, luciferase activity was detected with a dual-luciferase reporter gene system.

2.12. RNA immunoprecipitation (RIP) assay

The RIP assay was performed by using a Magna RIP RNA-Binding Protein Immunoprecipitation Kit (Millipore, USA). NP-40 lysis buffer containing 1 mmol/L PMSF, 1 mmol/L DTT, 1% protease inhibitor cocktail (Sigma-Aldrich) and RNase inhibitor (Invitrogen) was used to collect and lyse cells. Subsequently, the cells were incubated with RIP buffer containing magnetic beads bound with human anti-Argonaute2 (Ago2) antibody (Millipore) or normal mouse IgG (Millipore) as a negative control for 4 h at 4 °C. Finally, the precipitate was digested with Proteinase K buffer, and then co-immunoprecipitated RNA was isolated for qRT-PCR and miRNA RT-PCR analysis.

2.13. Western blot

As previously reported, total protein was extracted, subjected to 10% SDS–PAGE electrophoresis, and transferred to a sealed PVDF membrane. Then, the PVDF membrane was incubated overnight with specific antibodies, including CD81 (ab219209, 1:1000), TSG101 (ab125011, 1:5000) CD63 (ab134045, 1:2000), Calncxin (ab22595, 1:10000), PRDX2 (ab22595, 1:20000, 1:10000) and VEGF (ab32152, 1:2000), at 4 °C. The second day, after incubation with goat anti-rabbit IgG H&L (HRP) (ab6721, 1:5000), the bands were detected by a gel imaging system. GAPDH was used as the endogenous control. Abcam (Cambridge, United Kingdom) provided all antibodies.

2.14. Statistical analysis

The three replicates are represented as the mean ± standard deviation (SD). The *t*-test was used for the between-group comparison, and one-way ANOVA and Tukeys multiple comparisons were used for the between-group comparison. Univariate and multivariate Cox

proportional hazard analyses were used to calculate the Cox proportional hazard ratio between OS and PFS and clinical parameters. Statistical analyses were performed using SPSS 13.0 for Windows software (SPSS, Inc., Chicago, Illinois). P values were bilaterally tested, and $P < 0.05$ was considered to indicate a statistically significant difference.

3. Results

3.1. miR-23a-5p was downregulated in exosomes separated from the serum of HCC patients

First, exosomes were isolated from the serum of patients with HCC. Transmission electron microscopy (TEM) and dynamic light scattering (DLS) analysis showed that the exosomes were circular vesicles with a typical cup-like structure approximately 100 nm in diameter (Fig. 1A and B). Analysis indicated that the exosomal markers CD81 and TSG101 were highly expressed in exosomes (Fig. 1C, uncropped blots in Fig. S2). qRT−PCR analysis showed that the miR-23a-5p level 3 days after TACE was significantly higher than that before TACE, but the levels of miR-155-3p, miR-135b, miR-130b-3p and miR-210-3p did not change, and miR-23a-5p was downregulated in HCC tissues (Fig. 1D). In addition, as shown in Table 1 110 patients with HCC were divided into two groups: a low miR-23a-5p expression group (n = 52) and a high miR-23a-5p expression group (n = 58). Analysis indicated that there was no significant correlation between the level of miR-23a-5p and patient sex, age, tumor number, ALB or AFP level, whereas it was obviously related to maximum tumor size, BCLC stage, ALT, AST and PT (Table 1). Cox regression analyses also proved that the dysregulation of miR-23a-5p expression significantly increased the death risk (HR [95% CI] = 2.47 [1.83–3.35]) and tumor recurrence risk (HR [95% CI] = 2.05 [1.55–2.71]) (Table 3). In univariate analysis, BCLC stage, ALT, AST, PT, and preoperative miR-23a-5p expression were associated with PFS, and BCLC stage, ALT, PT, and postoperative miR-23a-5p expression significantly influenced OS. In multivariate analysis, BCLC stage, PT, and preoperative miR-23a-5p expression were independent prognostic factors of PFS, and BCLC stage, ALT, and preoperative miR-23a-5p expression were independent factors predicting OS (Tables 3 and 4). Moreover, compared with that in the control, miR-23a-5p was downregulated in HCC cell lines, especially in HepG2 and SKHep-1 cells (Fig. 1E). Therefore, HepG2 and SKHep-1 cells were used for follow-up functional studies. Overall, these data show that miR-23a-5p was significantly correlated with survival, and abnormal expression of miR-23a-5p significantly increased the risk of death and tumor recurrence. High expression of miR-23a-5p significantly inhibited tumor size and ALT and AST levels, shortened prothrombin time, and increased patient survival time.

3.2. miR-23a-5p carried by exosomes inhibited HCC cell proliferation and angiogenesis

To investigate the role of exosomal miR-23a-5p in HCC progression, HepG2 and SKHep-1 cells were cocultured with exosomes that were separated from the serum of HCC patients after 3 days of TACE and transfected with a miR-23a-5p inhibitor for miR-23a-5p

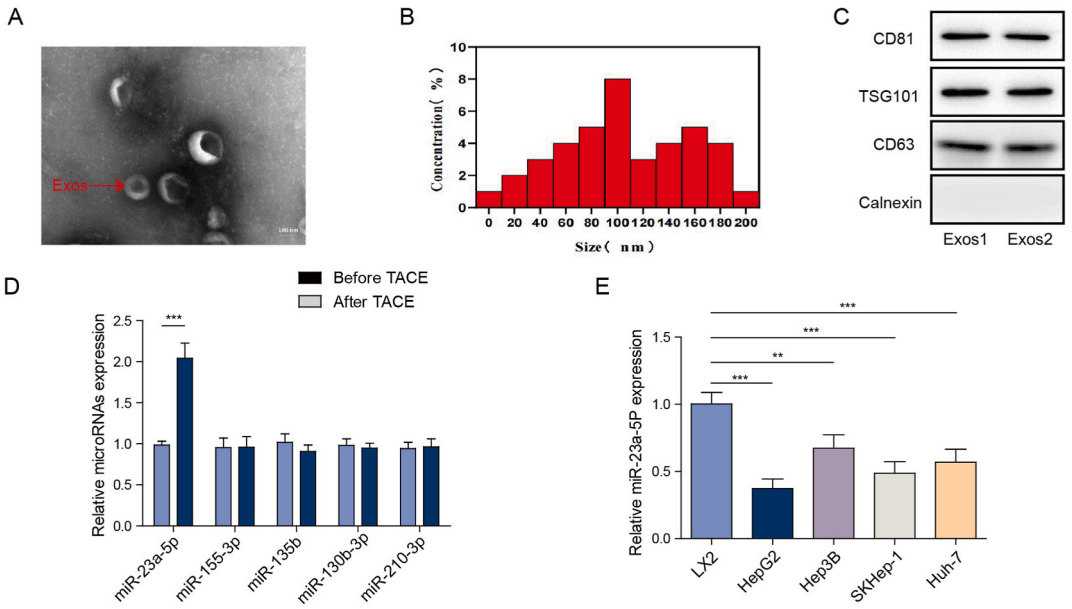

Fig. 1. miR-23a-5p was downregulated in exosomes separated from the serum of HCC patients. Exosomes were separated from the serum of HCC patients after 3 days of TACE. A, Exosome features were observed by TEM. B, Exosome diameter was observed by DLS. C, The expression of CD81, TSG101, CD63 and Calnexin in exosomes was evaluated by Western blotting. D, The levels of miR-23a-5p, miR-155-3p, miR-135b, miR-130b-3p and miR-210-3p in the serum of HCC patients 3 days after TACE were measured by qRT−PCR. E, miR-23a-5p levels in HCC cell lines, including HepG2, Hep3B, SKHep-1 and Huh-7, were measured by qRT−PCR, and LX2 cells served as the negative control. $^{**}P < 0.01$, $^{***}P < 0.001$.

Table 3
Univariate analysis of factors associated with OS and PFS.

Variables	OS		PFS	
	HR (95% CI)	P_{trend}	HR (95% CI)	P_{trend}
Gender (male, female)	0.89 (0.69–1.22)	0.43	0.95 (0.71–1.24)	0.51
Age (<60, ≥60)	0.86 (0.65–1.18)	0.37	0.77 (0.63–1.18)	0.28
Maximum tumor size (≤ 10 cm, >10 cm)	0.69 (0.51–0.94)	0.06	0.72 (0.55–0.98)	0.09
BCLC stage (A, B, C)	1.53 (1.31–1.92)	<0.001	1.59 (1.36–1.97)	<0.001
Tumor number(N) (1, >1)	0.97 (0.73–1.31)	0.92	0.91 (0.68–1.22)	0.41
ALT (U/L) (≤ 40, >40)	1.41 (1.09–1.88)	<0.001	1.33 (1.01–1.75)	0.03
AST (U/L) (≤ 40, > 40)	1.35 (1.02–1.76)	0.05	1.29 (1.09–1.68)	0.28
ALB (g/L) (≤ 35, > 35)	0.79 (0.58–1.07)	0.25	0.83 (0.51–1.09)	0.19
PT(s) (≤ 13, > 13)	1.35 (0.99–1.78)	<0.001	1.31 (0.95–1.72)	0.28
AFP(ng/ml) (≤ 20, 20–200, ≥ 200)	1.19 (0.91–1.57)	0.39	1.26 (0.95–1.68)	<0.001
Preoperative miR-23a-5p expression (high vs. low)	2.47 (1.83–3.35)	<0.001	2.05 (1.55–2.71)	

Table 4
Multivariate analysis of prognostic factors to predict OS and PFS.

Variables	HR (95% CI)	P_{trend}
OS		
BCLC stage (A, B, C)	1.41 (1.24–1.75)	<0.001
ALT (U/L) (≤40, >40)	1.33 (0.97–1.75)	0.031
Postoperative miR-23a-5p expression (high vs. low)	2.35 (2.01–3.16)	0.024
PFS		
BCLC stage (A, B, C)	1.48 (1.27–1.78)	0.002
PT(s) (≤13, >13)	1.45 (1.05–1.93)	0.046
Preoperative miR-23a-5p expression (high vs. low)	2.14 (1.66–2.89)	<0.001

inhibition. Normal cultured cells served as the negative control. qRT−PCR analysis showed that miR-23a-5p was upregulated in HepG2 and SKHep-1 cells after coculture with exosomes that were separated from the serum of HCC patients after 3 days of TACE, but the miR-23a-5p level was subsequently abolished by the miR-23a-5p inhibitor (Fig. 2A). Next, HepG2 and SKHep-1 cell viability and proliferation were both inhibited after coculture with exosomes that were separated from the serum of HCC patients after 3 days of TACE, whereas the downward trend was rescued by the miR-23a-5p inhibitor (Fig. 2B and C). Similarly, tube formation assays indicated that the number of tubules was significantly reduced after coculture with exosomes that were separated from the serum of HCC patients after 3 days of TACE, while the miR-23a-5p inhibitor reversed the decreasing trend (Fig. 2D). Moreover, ELISA analysis indicated that the levels of the oxidative stress markers MDA and SOD were significantly increased in HepG2 and SKHep-1 cells after coculture with exosomes that were separated from the serum of HCC patients after 3 days of TACE, but the levels of MDA and SOD were subsequently abolished by the miR-23a-5p inhibitor (Fig. 2E). As shown in Fig. 2F, the level of ROS was significantly increased in HepG2 and SKHep-1 cells after coculture with exosomes that were separated from the serum of HCC patients after 3 days of TACE, whereas the miR-23a-5p inhibitor inhibited ROS generation. In summary, we believe that miR-23a-5p carried by exosomes inhibits HCC cell proliferation and angiogenesis.

PRDX2 knockdown promoted oxidative stress and inhibited HCC cell proliferation and angiogenesis, and miR-23a-5p negatively targeted PRDX2.

To explore the potential downstream targets of miR-23a-5p, we found that PRDX2 may be a potential target gene of miR-23a-5p by bioinformatics software TargetScan analysis (Fig. 3A), and we designed the mutation site of PRDX2 targeted by miR-23a-5p (Fig. 3B). Then, a dual-luciferase reporter gene assay showed that the luciferase activity of the reported PRDX2-WT gene was inhibited by co-transfection of miR-23a-5p, but the luciferase activity of the reported PRDX2-MUT gene in HepG2 and SKHep-1 cells was not changed by co-transfection of miR-23a-5p (Fig. 3C). Subsequently, after RIP experiments (PMID: 30144184), we found that the levels of miR-23a-5p and PRDX2 in the complex increased significantly by using RT−qPCR detection, which further confirmed that miR-23a-5p targeted binding to miR-23a-5p (Fig. 3D). Moreover, analysis indicated that PRDX2 was significantly decreased in the serum of HCC patients after 3 days of TACE (Fig. 3E). Conversely, PRDX2 was significantly upregulated in HepG2 and SKHep-1 cells after transfection with the miR-23a-5p inhibitor (Fig. 3F). Furtherly, we explored in depth the effect of PRDX1 on oxidative stress in supplementary. In detail, we separately knocked down PRDX2 in HCC cells and simultaneously added a ROS inhibitor (*N*-Acetylcysteine, NAC) to detect cell proliferation, angiogenesis, and ROS level changes. qRT-PCR analysis indicated that the expression of PRDX2 decreased after knockdown of PRDX2, and the addition of ROS inhibitors did not affect the expression of PRDX2 (Fig. S1A). Western blot analysis showed that the expression of PRDX2 and VEGF decreased after knockdown of PRDX2. Meanwhile, the addition of ROS inhibitors did not affect the expression of PRDX2, but increased the expression of VEGF (Fig. S1B, uncropped blots in Fig. S2). As showing in Figs. S1C–1E, after knocking down PRDX2, cell viability, proliferation and angiogenesis were inhibited, but which were increased with the addition of ROS inhibitor. DCFH-DA staining showed that the intracellular ROS production was significantly increased after PRDX2 knockdown, and the addition of ROS inhibitors significantly inhibited ROS production (Fig. S1F). Moreover, we selected the HCC cell line HepG2 as the study object and overexpressed and knocked down miR-23a-5p in HepG2 cells to detect the

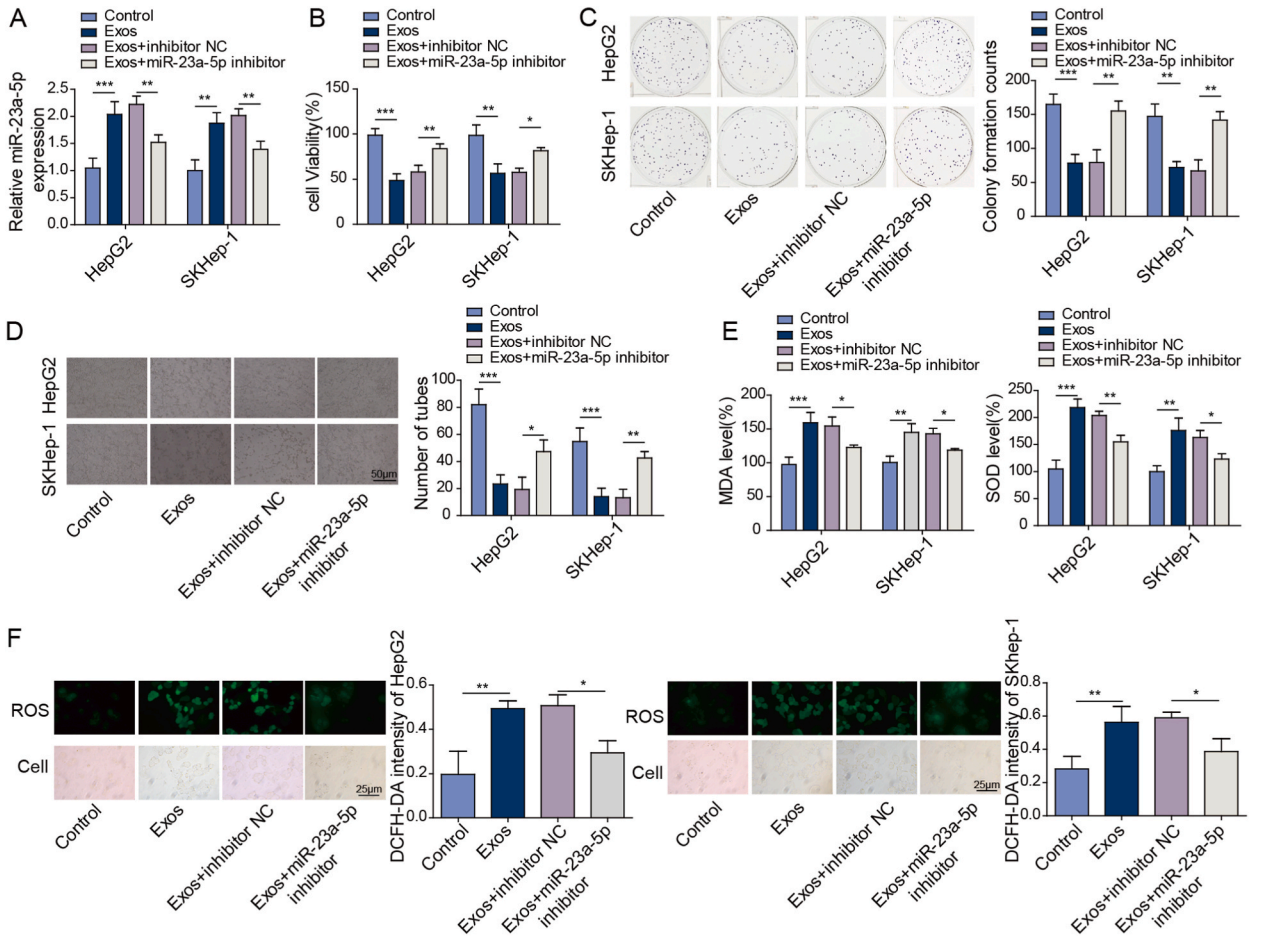

Fig. 2. MiR-23a-5p carried by exosomes inhibited HCC cell proliferation and angiogenesis. HepG2 and SKHep-1 cells were randomly divided into four groups. In the control group, the cells were cultured normally. In the Exo group, cells were cocultured with exosomes separated from the serum of HCC patients after 3 days of TACE. In the Exos + inhibitor NC group, cells were cocultured with exosomes separated from the serum of HCC patients after 3 days of TACE and transfected with inhibitor NC, which served as the negative control for the miR-23a-5p inhibitor. In the Exos + miR-23a-5p inhibitor group, cells were cocultured with exosomes separated from the serum of HCC patients after 3 days of TACE and transfected with miR-23a-5p inhibitor for miR-23a-5p inhibition. A, qRT−PCR measured miR-23a-5p levels in HepG2 and SKHep-1 cells. B, MTT assay detected HepG2 and SKHep-1 cell viability. C, Colony formation assay detected HepG2 and SKHep-1 cell proliferation. D, Tube formation assay detected tubule formation ability. E, ELISA measured the levels of MDA and SOD. F, DCFH-DA staining measured the level of ROS. $^{*}P < 0.05$, $^{**}P < 0.01$, $^{***}P < 0.001$.

effects on PRDX2 mRNA and protein levels. The results showed that the increase in PRDX2 expression inhibited by the miR-23a-5p inhibitor was reversed by miR-23a-5p mimics (Fig. 3G and H, uncropped blots in Fig. S2). Overall, we determined that miR-23a-5p negatively targets PRDX2.

PRDX2 overexpression relieved exosome-induced inhibition of HCC cell proliferation and angiogenesis by promoting VEGF expression.

To further survey the role and underlying molecular mechanism of PRDX2 in HCC progression, HepG2 and SKHep-1 cells were cocultured with exosomes separated from the serum of HCC patients after 3 days of TACE and transfected with oe-PRDX2 for PRDX2 overexpression. Normal cultured cells served as the negative control. Analysis indicated that PRDX2 was downregulated in HepG2 and SKHep-1 cells after coculture with exosomes that were separated from the serum of HCC patients after 3 days of TACE, but PRDX2 levels were subsequently rescued by oe-PRDX2 transfection (Fig. 4A). Analysis indicated that VEGF was significantly downregulated after coculture with exosomes that were separated from the serum of HCC patients after 3 days of TACE, while PRDX2 overexpression alleviated the inhibitory effect (Fig. 4B, uncropped blots in Fig. S2). Functionally, the cell viability and proliferation of HepG2 and SKHep-1 cells were inhibited after coculture with exosomes that were separated from the serum of HCC patients after 3 days of TACE, whereas the impact of exosomes was subsequently recovered by PRDX2 overexpression (Fig. 4C and D). Subsequently, tube formation assays indicated that the number of tubules was significantly reduced after coculture with exosomes that were separated from the serum of HCC patients after 3 days of TACE, but PRDX2 overexpression reversed the downward trend (Fig. 4E). Conversely, ELISA analysis indicated that the increase in MDA and SOD levels induced by exosomes separated from the serum of HCC patients after 3 days

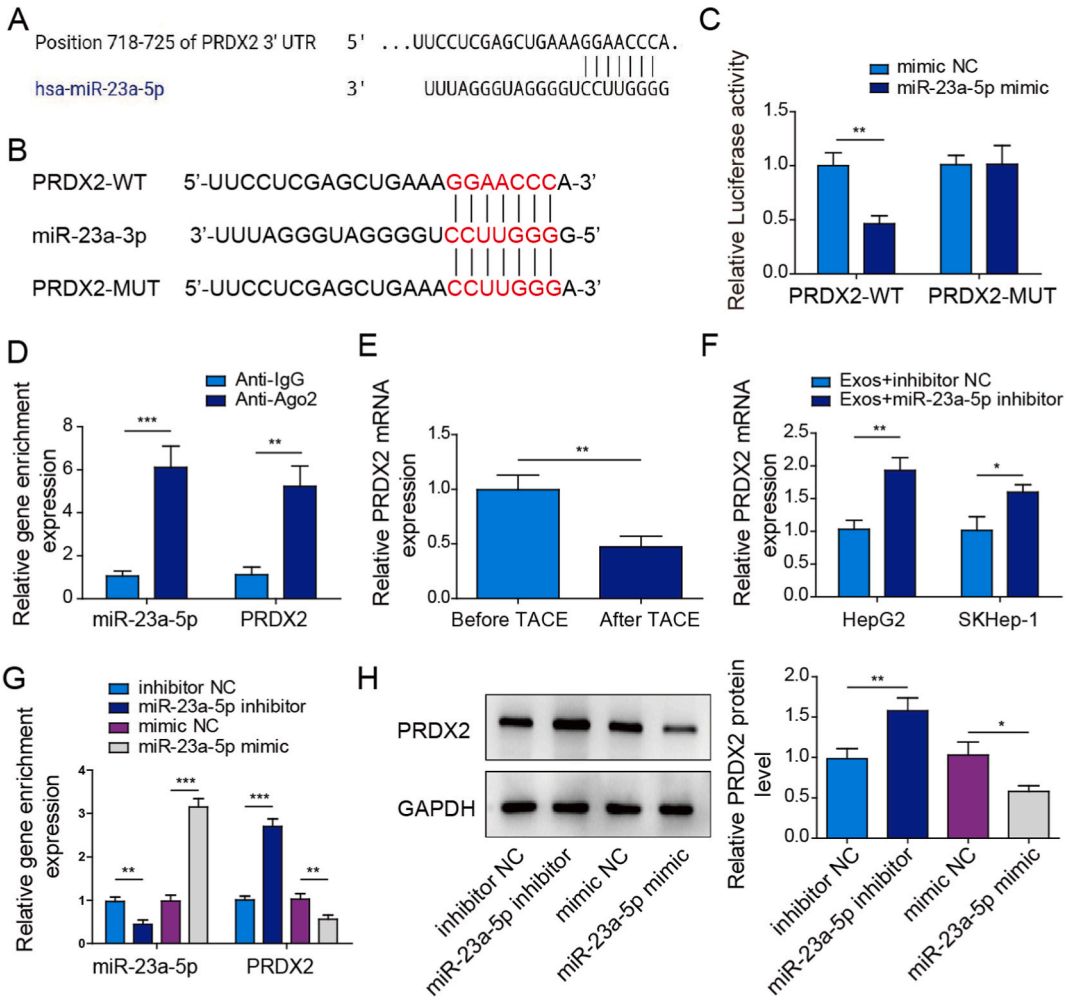

Fig. 3. PRDX2 knockdown promoted oxidative stress and inhibited HCC cell proliferation and angiogenesis, and miR-23a-5p negatively targeted PRDX2. A-B, Bioinformatics software TargetScan analysis showed that there were potential targets between PRDX2 and miR-23a-5p. C, A dual-luciferase reporter gene assay verified the targeting relationship between PRDX2 and miR-23a-5p. D, RIP assay further confirmed the targeting relationship between PRDX2 and miR-23a-5p. E, qRT−PCR was used to measure PRDX2 levels in the serum of HCC patients 3 days after TACE. F, qRT−PCR measured PRDX2 levels in HepG2 and SKHep-1 cells after transfection with miR-23a-5p inhibitor. G, qRT−PCR was used to measure PRDX2 levels in HepG2 and SKHep-1 cells after transfection with miR-23a-5p mimics. H, Western blot analysis of PRDX2 levels in HepG2 and SKHep-1 cells after transfection with miR-23a-5p mimics. $^{*}P < 0.05$, $^{**}P < 0.01$, $^{***}P < 0.001$.

of TACE was abolished by PRDX2 overexpression (Fig. 4F). Furthermore, the increase in ROS levels induced by exosomes separated from the serum of HCC patients after 3 days of TACE was inhibited by PRDX2 overexpression (Fig. 4G). Therefore, we concluded that PRDX2 overexpression relieved exosome-induced inhibition of HCC cell proliferation and angiogenesis by promoting VEGF expression.

4. Discussion

Cancer cells and surrounding tumor mechanisms constitute the malignant tumor microenvironment [21]. Increasing evidence shows that exosomes play a pivotal role in the local and systemic intercellular communication of cancer [22]. Our findings illustrated that exo miR-23a-5p inhibited HCC proliferation and angiogenesis by regulating PRDX2 expression. Our study demonstrated,the effect and specific molecular mechanism of exo miR-23a-5p in regulating HCC progression.

Tumor-derived exosomes play an important role in the construction of the tumor growth microenvironment, including promoting tumorigenesis, invasion and metastasis [5]. As small vesicle structures secreted by cells, exosomes have a long half-life in circulation and can provide a relatively safe environment for a variety of bioactive substances to ensure that the bioactive substances can be effectively transported into the receptor cells and play a role [23]. In this study, exosomes were successfully separated from the serum of HCC patients. Furthermore, we found that the miR-23a-5p level 3 days after TACE was significantly higher than that before TACE in the serum of HCC patients but significantly downregulated in HCC cell lines, including HepG2, Hep3B, SKHep-1 and Huh-7, especially

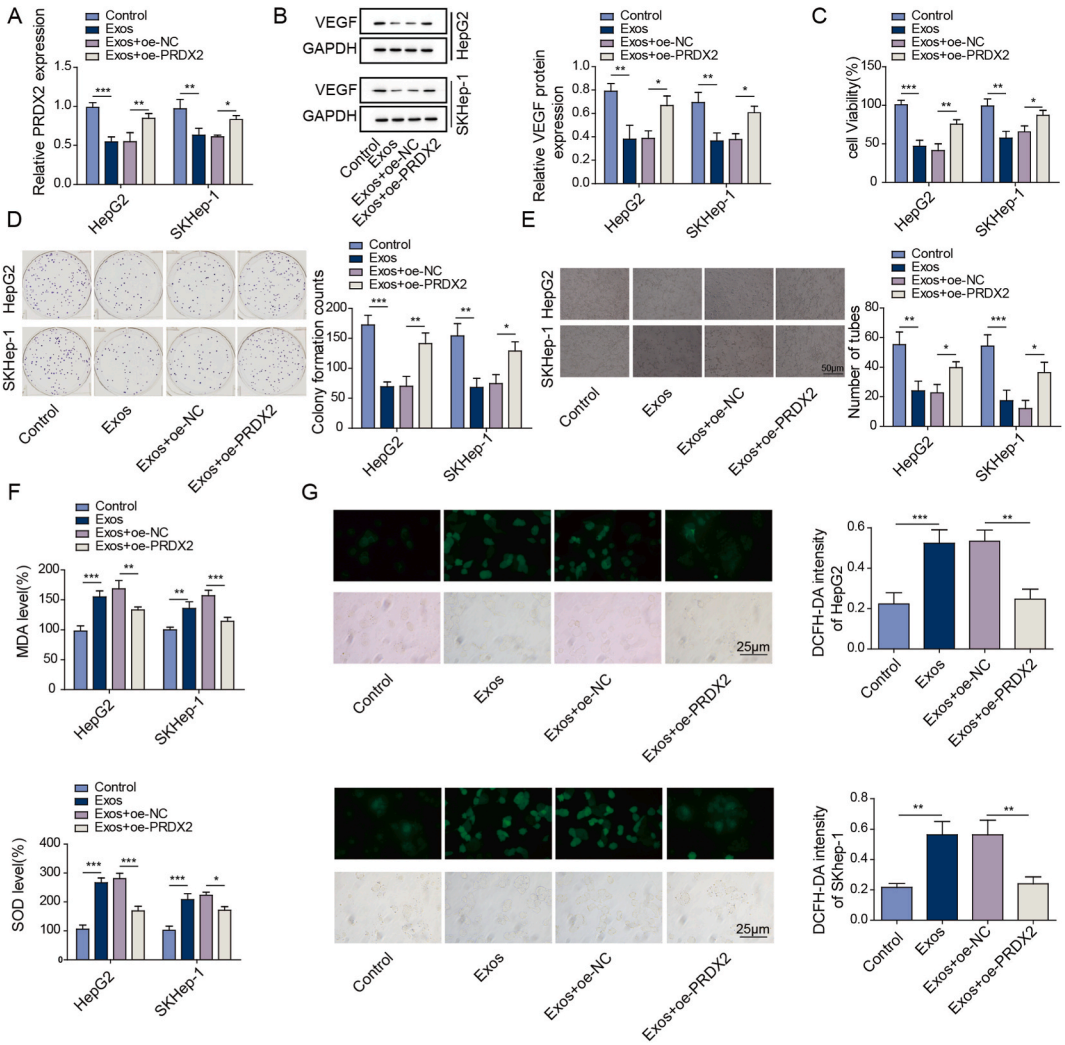

Fig. 4. PRDX2 overexpression relieved exosome-induced inhibition of HCC cell proliferation and angiogenesis by promoting VEGF expression. HepG2 and SKHep-1 cells were randomly divided into four groups. In the control group, the cells were cultured normally. In the Exo group, cells were cocultured with exosomes separated from the serum of HCC patients after 3 days of TACE. In the Exo + oe-NC group, cells were cocultured with exosomes separated from the serum of HCC patients after 3 days of TACE and transfected with oe-NC, which served as the negative control for oe-PRDX2. In the Exos + oe-PRDX2 group, cells were cocultured with exosomes separated from the serum of HCC patients after 3 days of TACE and transfected with oe-PRDX2 for PRDX2 overexpression. A, qRT−PCR was used to measure PRDX2 mRNA levels. B, Western blot analysis of VEGF protein levels. C, MTT assay detected HepG2 and SKHep-1 cell viability. D, Colony formation assay detected HepG2 and SKHep-1 cell proliferation. E, Tube formation assay detected tubule formation ability. F, ELISA measure the levels of MDA and SOD. G, DCFH-DA staining measured the level of ROS. $^{*}P < 0.05$, $^{**}P < 0.01$, $^{***}P < 0.001$.

in HepG2 and SKHep-1 cells. Moreover, the median PFS time was 8 months (range: 3–17), and the median OS was 14 months (range: 4–18) in this study. In univariate analysis, BCLC stage, ALT, AST, PT, and preoperative miR-23a-5p expression were associated with PFS, and BCLC stage, ALT, PT, and preoperative miR-23a-5p expression significantly influenced OS. In multivariate analysis, BCLC stage, PT, and preoperative miR-23a-5p expression were independent prognostic factors of PFS, and BCLC stage, ALT, and preoperative miR-23a-5p expression were independent factors predicting OS. Functionally, our findings revealed that miR-23a-5p carried by exosomes inhibited HCC cell proliferation and angiogenesis. These findings suggested that exo miR-23a-5p may play a negative role in HCC progression.

It has been reported that miRNAs are involved in regulating tumor development, including cell proliferation and angiogenesis, and may become new and effective therapeutic targets [24]. Notably, miR-23a-5p is involved in the regulation of the progression of multiple diseases by targeting tumor-associated genes. It has been reported that miR-23a-5p is involved in the regulation of pancreatic cancer by regulating the expression of ECM1 [25]. Zhou et al. found that miR-23a-5p participated in the malignant phenotype of cervical cancer cells by targeting SLC7A11 [26]. Specifically, Yang et al. showed that miR-23a-5p expression was downregulated in hepatoma cell lines and tissues and that miR-23a-5p regulated the progression of liver cancer by targeting IGF2 [16]. Similarly, our

results showed that miR-23a-5p negatively targeted PRDX2.

PRDX2 is a typical 2-cysteine peroxidation–reduction protein that has been shown to be induced by oxidative stress, and PRDX2 overexpression protects cells from oxidative damage [27]. Studies have also shown that upregulation of PRDX2 is associated with tumor progression and can be used as an effective biomarker for cancer prognosis [17]. For example, high expression of PRDX2 is associated with the proliferation and metastasis of non-small cell lung cancer cells [28]. In addition, Wang et al. indicated that PRDX2 can prevent oxidative stress induced by *Helicobacter pylori* and increase the tolerance of gastric cancer cells to cisplatin [29]. Interestingly, Zhou et al. reported that PRDX2 protected SMMC-7721 cells from oxidative stress in HCC [19]. Consistently, our results indicated that PRDX2 was significantly upregulated in the serum of HCC patients 3 days after TACE, indicating that PRDX2 may play a positive role in HCC progression. Moreover, the increase in MDA, SOD and ROS levels induced by exosomes separated from the serum of HCC patients after 3 days of TACE was abolished by PRDX2 overexpression, suggesting that PRDX2 overexpression protected HepG2 and SKHep-1 cells from oxidative stress in HCC. Functionally, PRDX2 overexpression relieved exosome-induced inhibition of HCC cell proliferation and angiogenesis by promoting VEGF expression. Overall, PRDX2 overexpression promoted HCC cell proliferation and angiogenesis by protecting HepG2 and SKHep-1 cells from oxidative stress.

In summary, exosomes adjust the tumor microenvironment by changing the physiological state of target cells. Therefore, exosomes are vital messengers in tumor progression. In this study, our findings illustrated that exo miR-23a-5p inhibited HCC proliferation and angiogenesis by regulating PRDX2 expression. Our study demonstrated, the role and specific molecular mechanism of exo miR-23a-5p in regulating HCC progression. Unfortunately, we did not study the specific mechanism of PRDX2-induced HCC cell proliferation and angiogenesis; in follow-up experiments, we will further study the relationship between PRDX2-induced HCC cell proliferation and angiogenesis.

Data availability statement

Data will be made available on request.

Ethics approval statement

All the protocols were approved by the Ethics Committee of Hunan Cancer Hospital, The Affiliated Cancer Hospital of Xiangya School of Medicine, Central South University (Protocol 2022(SRL)76). All methods were carried out in accordance with relevant guidelines and regulations. Research involving human participants, human material, or human data is conducted in accordance with the Declaration of Helsinki. The authors confirmed that informed consent was obtained from all subjects.

Patient consent statement

The authors confirmed that informed consent was obtained from all subjects.

CRediT authorship contribution statement

Yang Zhao: Writing – review & editing, Writing – original draft, Resources, Methodology, Conceptualization. **Jun Liu:** Writing – review & editing, Writing – original draft, Resources, Methodology, Conceptualization. **Zhengping Xiong:** Writing – review & editing, Writing – original draft, Supervision, Investigation, Formal analysis. **Shanzhi Gu:** Writing – review & editing, Supervision, Investigation. **Xibin Xia:** Writing – review & editing, Supervision, Investigation.

Declaration of competing interest

The authors declare that they have no known competing financial interests or personal relationships that could have appeared to influence the work reported in this paper.

Acknowledgements

This work has been supported by The Natural Science Foundation of Hunan Province (Grant Number: 2021JJ30423, Changsha, China), Hunan Cancer Hospital Climb Plan (Grant Number: ZX2020002-4, Changsha, China).

Abbreviations

miRNAs	microRNAs
HCC	Hepatocellular carcinoma
TACE	Transcatheter arterial chemoembolization
PRDX2	Peroxiredoxin-2
ELISA	Enzyme-linked immunosorbent assay
MDA	Malondialdehyde
SOD	Superoxide dismutase

DCFH-DA 2′,7′-dichlorodihydrofluorescein diacetate
ROS Reactive oxygen species
RIP RNA binding protein immunoprecipitation
TEM Transmission electron microscopy
DLS Dynamic light scattering
exo miR-23a-5p Exosome microRNA-23a-5p
VEGF Vascular endothelial growth factor
OS Overall survival
PFS Progression-free survival
AASLD American Association for the Study of Liver Disease
BCLC Barcelona clinic liver cancer
HUVECs Human umbilical vein endothelial cells

Appendix A. Supplementary data

Supplementary data to this article can be found online at https://doi.org/10.1016/j.heliyon.2023.e23168.

References

[1] B. Yang, X. Feng, H. Liu, et al., High-metastatic cancer cells derived exosomal miR92a-3p promotes epithelial-mesenchymal transition and metastasis of low-metastatic cancer cells by regulating PTEN/Akt pathway in hepatocellular carcinoma, Oncogene 39 (42) (2020) 6529–6543.
[2] A. Sorop, D. Constantinescu, F. Cojocaru, et al., Exosomal microRNAs as biomarkers and therapeutic targets for hepatocellular carcinoma, Int. J. Mol. Sci. 22 (9) (2021).
[3] Y. Zhou, H. Ren, B. Dai, et al., Hepatocellular carcinoma-derived exosomal miRNA-21 contributes to tumor progression by converting hepatocyte stellate cells to cancer-associated fibroblasts, J. Exp. Clin. Cancer Res. 37 (1) (2018) 324.
[4] M. Fu, J. Gu, P. Jiang, et al., Exosomes in gastric cancer: roles, mechanisms, and applications, Mol. Cancer 18 (1) (2019) 41.
[5] H. Kahroba, M.S. Hejazi, N. Samadi, Exosomes: from carcinogenesis and metastasis to diagnosis and treatment of gastric cancer, Cell. Mol. Life Sci. 76 (9) (2019) 1747–1758.
[6] X.W. Guan, F. Zhao, J.Y. Wang, et al., Tumor microenvironment interruption: a novel anti-cancer mechanism of Proton-pump inhibitor in gastric cancer by suppressing the release of microRNA-carrying exosomes, Am. J. Cancer Res. 7 (9) (2017) 1913–1925.
[7] T. Deng, H. Zhang, H. Yang, et al., Retraction notice to: exosome miR-155 derived from gastric carcinoma promotes angiogenesis by targeting the c-MYB/VEGF Axis of endothelial cells, Mol. Ther. Nucleic Acids 28 (2022) 16.
[8] H. Ohzawa, Y. Kumagai, H. Yamaguchi, et al., Exosomal microRNA in peritoneal fluid as a biomarker of peritoneal metastases from gastric cancer, Ann. Gastroenterol. Surg. 4 (1) (2020) 84–93.
[9] L. Chang, H. Gao, L. Wang, et al., Exosomes derived from miR-1228 overexpressing bone marrow-mesenchymal stem cells promote growth of gastric cancer cells, Aging (Albany NY) 13 (8) (2021) 11808–11821.
[10] X. Xia, S. Wang, B. Ni, et al., Hypoxic gastric cancer-derived exosomes promote progression and metastasis via MiR-301a-3p/PHD3/HIF-1α positive feedback loop, Oncogene 39 (39) (2020) 6231–6244.
[11] J. Liu, S. Wu, X. Zheng, et al., Immune suppressed tumor microenvironment by exosomes derived from gastric cancer cells via modulating immune functions, Sci. Rep. 10 (1) (2020), 14749.
[12] M. Xie, T. Yu, X. Jing, et al., Exosomal circSHKBP1 promotes gastric cancer progression via regulating the miR-582-3p/HUR/VEGF axis and suppressing HSP90 degradation, Mol. Cancer 19 (1) (2020) 112.
[13] Y. Tian, Y. Xing, Z. Zhang, et al., Bioinformatics analysis of key genes and circRNA-miRNA-mRNA regulatory network in gastric cancer, BioMed Res. Int. 2020 (2020), 2862701.
[14] X. Xu, F. Gao, J. Wang, et al., MiR-122-5p inhibits cell migration and invasion in gastric cancer by down-regulating DUSP4, Cancer Biol. Ther. 19 (5) (2018) 427–435.
[15] S. Zhao, Y. Mi, B. Guan, et al., Tumor-derived exosomal miR-934 induces macrophage M2 polarization to promote liver metastasis of colorectal cancer, J. Hematol. Oncol. 13 (1) (2020) 156.
[16] J. Yang, Y. Li, Z. Yu, et al., Circular RNA Circ100084 functions as sponge of miR-23a-5p to regulate IGF2 expression in hepatocellular carcinoma, Mol. Med. Rep. 21 (6) (2020) 2395–2404.
[17] L. Peng, R. Wang, J. Shang, et al., Peroxiredoxin 2 is associated with colorectal cancer progression and poor survival of patients, Oncotarget 8 (9) (2017) 15057–15070.
[18] S. Pérez, R. Taléns-Visconti, S. Rius-Pérez, et al., Redox signaling in the gastrointestinal tract, Free Radic. Biol. Med. 104 (2017) 75–103.
[19] S. Zhou, Q. Han, R. Wang, et al., PRDX2 protects hepatocellular carcinoma SMMC-7721 cells from oxidative stress, Oncol. Lett. 12 (3) (2016) 2217–2221.
[20] X. Jin, C. Chen, D. Li, et al., PRDX2 in myocyte hypertrophy and survival is mediated by TLR4 in acute infarcted myocardium, Sci. Rep. 7 (1) (2017) 6970.
[21] M. Sund, R. Kalluri, Tumor stroma derived biomarkers in cancer, Cancer Metastasis Rev. 28 (1–2) (2009) 177–183.
[22] L. Balaj, R. Lessard, L. Dai, et al., Tumour microvesicles contain retrotransposon elements and amplified oncogene sequences, Nat. Commun. 2 (2011) 180.
[23] P. Zheng, L. Chen, X. Yuan, et al., Exosomal transfer of tumor-associated macrophage-derived miR-21 confers cisplatin resistance in gastric cancer cells, J. Exp. Clin. Cancer Res. 36 (1) (2017) 53.
[24] A. Pennathur, T.E. Godfrey, J.D. Luketich, The molecular biologic basis of esophageal and gastric cancers, Surg. Clin. North Am. 99 (3) (2019) 403–418.
[25] W. Huang, Y. Huang, J. Gu, et al., miR-23a-5p inhibits cell proliferation and invasion in pancreatic ductal adenocarcinoma by suppressing ECM1 expression, Am. J. Transl. Res. 11 (5) (2019) 2983–2994.
[26] X. Zhou, X. Zhao, Z. Wu, et al., LncRNA FLVCR1-AS1 mediates miR-23a-5p/SLC7A11 axis to promote malignant behavior of cervical cancer cells, Bioengineered 13 (4) (2022) 10454–10466.
[27] S.W. Kang, I.C. Baines, S.G. Rhee, Characterization of a mammalian peroxiredoxin that contains one conserved cysteine, J. Biol. Chem. 273 (11) (1998) 6303–6311.
[28] Y. Chen, S. Yang, H. Zhou, et al., PRDX2 promotes the proliferation and metastasis of non-small cell lung cancer in vitro and in vivo, BioMed Res. Int. 2020 (2020), 8359860.
[29] S. Wang, Z. Chen, S. Zhu, et al., PRDX2 protects against oxidative stress induced by H. pylori and promotes resistance to cisplatin in gastric cancer, Redox Biol. 28 (2020), 101319.